Photoinduced Intramolecular Charge Transfer in Push−Pull Polyenes: Effects of Solvation, Electron-Donor Group, and Polyenic Chain Length †

ARTICLE *in* THE JOURNAL OF PHYSICAL CHEMISTRY B · FEBRUARY 2008

Impact Factor: 3.3 · DOI: 10.1021/jp075418z · Source: PubMed

5 AUTHORS, INCLUDING:

Damien Laage
Ecole Normale Supérieure de Paris
49 PUBLICATIONS **2,013** CITATIONS

Photoinduced Intramolecular Charge Transfer in Push−Pull Polyenes: Effects of Solvation, Electron-Donor Group, and Polyenic Chain Length†

Walther Akemann,[⊥,#] Damien Laage,[‡] Pascal Plaza,[‡] Monique M. Martin,*[,‡] and Mireille Blanchard-Desce[§]

UMR CNRS 8640, Département de Chimie, Ecole Normale Supérieure, 24 rue Lhomond, 75005 Paris, France, and UMR CNRS 6510, Synthèse et Electrosynthèse Organique, Université de Rennes 1, Campus de Beaulieu, Case 1003, 35042 Rennes Cedex, France

Received: July 11, 2007; In Final Form: September 18, 2007

Subpicosecond absorption spectroscopy is used to characterize the primary photoinduced processes in a class of push−pull polyenes bearing a julolidine end group as the electron donor and a diethylthiobarbituric acid end group as the electron acceptor. The excited-state decay time and relaxation pathway have been studied for four polyenes of increasing chain length ($n = 2-5$ double bonds) in aprotic solvents of different solvation time, polarity, and viscosity. Intramolecular charge transfer (ICT) leading to a transient state of cyanine-like structure (fully conjugated with no bond length alternation) is observed in all polar solvents at a solvent dependent rate, but the reaction is not observed in cyclohexane, a nonpolar solvent. In polar solvents, the reaction time increases with the average solvation time but remains slightly larger, except in the viscous solvent triacetin. These facts are interpreted as an indication that both solvent reorganization and internal restructuring are involved in the ICT-state formation. The observed photodynamics resemble those we previously found for another class of polyenes bearing a dibutylaniline group as the donor, including a similar charge-transfer rate in spite of the larger electron donor character of the julolidine group. This observation brings further support to the proposal that an intramolecular coordinate is involved in the charge-transfer reaction, possibly a torsional motion of the donor end group. On the other hand, relaxation of the ICT state leads to cis−trans isomerization or crossing to the triplet state, depending on the length of the polyenic chain. In dioxane, tetrahydrofuran, and triacetin, the ICT state of the shorter chains ($n = 2, 3$) relaxes to the isomer with a viscosity-dependent rate, while that of the longer ones ($n = 4, 5$) leads to the triplet state with a viscosity-independent rate, as expected. In acetonitrile, the ICT-state lifetime is generally much shorter. A change from photoisomerization to intersystem crossing at $n = 4$ is also proposed in this solvent, but the formation of a photoproduct at $n = 2$ is not clear. In cyclohexane, where the ICT state is not formed, the relaxation pathway of the initially excited state is found to lead to an isomer for $n = 2$. As in polar solvents, a change to intersystem crossing at $n = 4$ is proposed. The direct relaxation to the ground state found at $n = 3$ for the series bearing a dibutylaniline group is not observed with the julolidine group. The results clearly illustrate that photoinduced reaction trajectories in push−pull polyenes are controlled by the static and dynamic properties of the solvent, the chemical nature and size of the end groups, and the conjugated-chain length and flexibility.

1. Introduction

Interaction of light with electron donor−acceptor (EDA) π-conjugated systems is of primary importance in the search for optical materials based on organic molecules. EDA compounds are often involved in supramolecular devices capable of performing useful photoinduced functions, such as fluorescent sensing for ions or molecules, solar energy conversion or optical information storage. Substituted polyenes are involved in various aspects of photoabsorption and charge-carrier generation. Extensive research has been carried out on polymethine cyanine dyes for high-density optical recording.[1,2] Carotenoids have been the object of active research aimed at understanding and mimicking natural photosynthesis.[3−5] The most common biological photoreceptors involved in vision and archaeal photosynthesis, rhodopsins and bacteriorhodopsins, rely on photoinduced processes in retinal.[6−10] Push−pull polyenes with EDA end groups have received much attention because they are highly polarizable[11−23] and thus promising compounds for nonlinear optics, harmonics generation, optical limitation, two-photon absorption, and optical imaging of biological materials.[24−29]

In the present paper, we report on light-induced processes in a class of push−pull polyenes designed to manifest large quadratic and cubic hyperpolarizabilities.[30−32] They have been studied for their nonlinear optical properties both experimentally and theoretically,[30−35] but little is known on their fundamental photophysical properties.[36−38] We previously demonstrated that optical excitation of a series of push−pull polyenes, bearing a dibutylaniline donor group and a diethylthiobarbituric acid

† Part of the "James T. (Casey) Hynes Festschrift".

* Corresponding author. E-mail: monique.martin@ens.fr. Phone +33 (0)1.44.32.24.12. Fax +33 (0)1.44.32.33.25.

‡ Ecole Normale Supérieure.

§ Université de Rennes 1.

⊥ Postdoctoral fellow in M.M. Martin's group at the Laboratoire de Photophysique Moléculaire du CNRS at Orsay University.

Present address: Laboratory for Neuronal Circuit Dynamics, RIKEN Brain Science Institute 2-1 Hirosawa, Wako-City, Saitama 351-0198, Japan.

10.1021/jp075418z CCC: $40.75
Published on Web 11/13/2007

SCHEME 1: Chemical Structure of the PA_n and PB_n (n = 2 to 5) Push−Pull Polyenes[a]

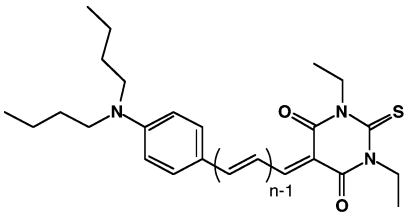

PA_n

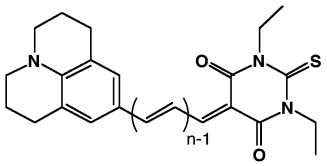

PB_n

[a] Both have a diethylthiobarbituric acid group as the electron acceptor. In PA_n, the electron donor is a dibutylaniline, and, in PB_n, it is a julolidine.

acceptor group (Scheme 1, PA_n) in polar solvents, leads to the ultrafast formation of an intramolecular charge transfer (ICT) state, bringing support to the proposal that a proper description of their excited-state dynamics requires more than two valence bond states.[36] The ICT-state gain spectra were found to exhibit a regular 100-nm shift per added double bond in the polyenic chain ($n = 2-5$ double bonds). A photoinduced charge transfer with geometrical change toward the formation of a transient state with a rigid, fully conjugated cyanine-like structure was suggested to occur in polar solvents.[36] In a detailed comparative study of the PAs in dioxane and cyclohexane by subpicosecond transient absorption spectroscopy,[38] we demonstrated that the relaxation pathway, leading to the ICT state only in dioxane, is first determined by the solvent polarity for ultrashort times (2−3 ps), then by the polyenic chain length for longer times with a pathway change for $n = 3$. Photoisomerization occurs for $n = 2$, whereas intersystem crossing to the triplet state occurs for $n = 4$. For $n = 3$, the triplet state is observed in dioxane, while an intermediate regime with a relaxation back to the ground state is found in cyclohexane. We therefore stressed the importance of characterizing the parameters influencing the photoinduced reaction trajectories in these push−pull polyenes.[38]

Here we focus on the photophysical and photochemical properties of the series bearing a julolidine instead of a dibutylaniline moiety, that is, a stronger and more compact electron donor end group (Scheme 1, PB_n).[30,31] We studied the excited-state decay time and relaxation pathway of four such polyenes (n ranging from 2 to 5) and compared them to the corresponding PA_n. The photodynamics of PB_n in a series of polar and nonpolar solvents has been followed in real time by subpicosecond transient absorption spectroscopy. Additional data are also provided for the PA_n series. The roles of solvation and internal torsion coordinates in the relaxation pathway are examined and discussed on the basis of the Kim−Hynes model,[39] developed for the formation of a twisted intramolecular charge transfer (TICT) state in dimethylaminobenzonitrile (DMABN), and on the basis of the Grote−Hynes model[40] for solvent viscosity effects. The effect of solvent and chain length on the relaxation mechanism and nature of the long-lived photoproduct are also examined, emphasizing the occurrence of multiple relaxation pathways in this class of compounds. The similarity between the ultrafast dynamics of PA_n and PB_n and phenomena reported for peridinin,[5,41−47] which plays an important role in photosynthesis, is of primary importance for the understanding of the complex excited-state behavior of natural carbonyl carotenoids.

2. Experimental Section

Transient absorption spectra were measured by the pump−probe technique using ∼0.5 ps, 20−40 μJ pump pulses at 570−572 or 610 nm, provided by a dye-laser system according to unconventional methods described elsewhere.[48] The pump-continuum probe setup was the same as that used in ref 36. The sample cell provided an optical path length of 1 mm. The pump and probe beams had a diameter of about 1 mm when superimposed within the sample with a relative angle of ∼10°. The transmitted probe beam and a second probe beam going through a reference cell were guided through 2.50-m long optical fibers to the 64-μm entrance slit of a spectrograph (Spex 270M). The spectra of the two probe beams were simultaneously recorded by a computer-controlled double-diode array detector (Princeton Instruments, Inc. DDA-512). The pump−probe delay time was adjusted by means of a stepper motor translation (Microcontrole M-MTM250PP1), which allowed delays up to ∼1.7 ns. Pump and probe beam polarizations were set at the magic angle. Data were accumulated over 500 or 1000 pump shots. A few pump−probe experiments were carried out with pump−probe delays extending up to several tens of milliseconds by using two synchronized subpicosecond dye-lasers, one used as the pump and the other for continuum-probe generation.[38]

The design, synthesis, and purification procedures of the push−pull polyenes were described in ref 30. UV-spectroscopy-grade (Merck, Uvasol) cyclohexane, dioxane, tetrahydrofuran (THF), and acetonitrile were used as the solvents. Triacetin (glycerol triacetate, Aldrich) was chosen as a viscous solvent, and its quality was checked by fluorescence spectroscopy. The solutions were not deaerated and were used immediately after preparation or after up to 3 days of storage at −27 °C. The solute concentration was adjusted to have an absorbance of 0.3−1 at the excitation wavelength, depending on its solubility, and the solutions were recirculated. The experiments were carried out at room temperature.

3. Results

3.1. Picosecond Transient Absorption Spectra in a Nonpolar Solvent, Cyclohexane. The differential absorption spectra (ΔA) measured for the four PB_n dissolved in cyclohexane, upon subpicosecond excitation at 572 nm ($n = 2, 3$) or 610 nm ($n = 4, 5$), are displayed in Figure 1. One can note that the ground-state absorption spectrum (also recalled in Figure 1) of PB_2 exhibits a maximum at 565 nm and a shoulder around 540 nm, while the spectra of $PB_{3,4,5}$ display a broad band around 600 nm with blurred structures, especially for the longest chains. In all cases, the differential absorption spectra at the end of the excitation pulse are composed of a transient absorption band ($\Delta A > 0$) on the blue side of the ground-state absorption spectrum, and a stimulated-emission band ($\Delta A < 0$) on its red side. Between them, one can identify the bleaching band ($\Delta A < 0$ in the region of the ground-state absorption). In the four cases, once the transient absorption and stimulated-emission bands have decayed, a new absorption band in the red side of the ground-state absorption remains. The best fit of the observed $\Delta A(t)$ was obtained by convoluting the pump−probe cross-correlation function (assumed to be a Gaussian) with the sum of one exponential and a step function describing the residual

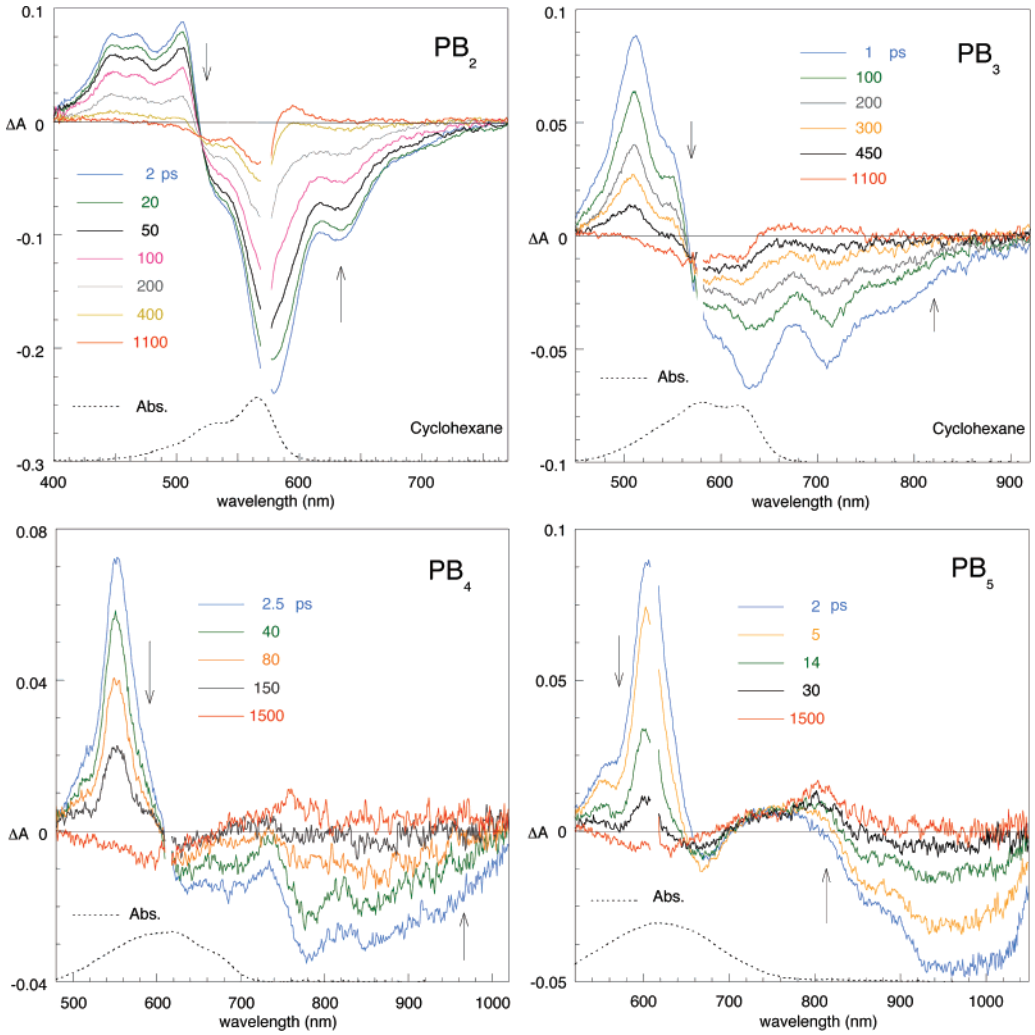

Figure 1. Differential absorption (ΔA) spectra of the PB_n polyenes in cyclohexane, upon subpicosecond excitation at 572 nm ($n = 2, 3$) or 610 nm ($n = 4, 5$). Scattered light from the excitation laser has been masked. The ground-state absorption spectrum is shown as a dotted line. The arrows indicate the evolution of bands with increasing time.

signal at long delays. This analysis yielded time constants of 160, 230, 120, and 12 ps, respectively, for $n = 2-5$. The values are given in Table 1, together with those observed for the PA_n series.[38] The residual absorption observed at 1.5 ns, the longest pump−probe delay allowed by our setup, is accompanied by a residual bleaching. A few experiments carried out up to the millisecond time range are described in section 3.4.

3.2. Picosecond Transient Absorption Spectra in Low-Viscosity Polar Solvents. Pump−probe experiments have been carried out on the four PB_n in three solvents of increasing polarity: dioxane, THF, and acetonitrile. In Table 1, their polarity is described by the dielectric constant and the π^* empirical parameter[49] (microscopic solvation properties of the nondipolar dioxane[50] are better described by π^*). Their viscosity and average solvation times are also given. The average solvation times, which include both the inertial and diffusive part of the solvation dynamics, are taken from the work of Horng et al.[51]

Dioxane. The differential absorption spectra of the four compounds upon subpicosecond excitation at ~570 nm are shown in Figure 2 together with the ground-state absorption of the samples. There is a slight red shift of the ground-state absorption of PB_2 and PB_3 compared to those in cyclohexane (Figure 1), whereas the spectra of PB_4 and PB_5 remain in the same spectral range. The spectra are broad, and a residual structure is hardly visible even for the short chains. Like in cyclohexane, the short-time differential absorption spectra are composed of the characteristic absorption, bleaching, and stimulated-emission bands. The time-resolved changes, however, involve additional short-time dynamics. A temporary isosbestic point (with nonzero ΔA value, which will be called TIP) is observed in the stimulated-emission band within a few picoseconds after excitation, around 635, 716, 795, and 850 nm, respectively, for $n = 2-5$. This TIP results from an increase in the amplitude of the stimulated-emission band with the concomitant decay of the ΔA signal in the long wavelength tail of the bleaching band. The delayed increase of the stimulated emission has a larger amplitude for longer chains. For PB_4 and PB_5, this short-time spectral evolution also reveals the presence of a transient absorption band around 720 and 780 nm, respectively, which further evolves into a broad and flat absorption band, respectively centered around 780 and 840 nm. This further evolution is concomitant to the decay of the stimulated-emission band. For PB_2 and PB_3, since the stimulated-emission band has not completely vanished at 1.5 ns, a simple examination of the spectra does not allow for deciding whether a photoproduct is formed or not. The TIP observed in the bleaching band of PB_3 around 575 nm is nevertheless an indication that the excited-state relaxation leads to a species different from the ground state. The fit of the time-resolved differential absorption was done at several wavelengths by convoluting the pump−probe cross-correlation function with a

TABLE 1: Averaged[a] Time Components τ_i (in Picoseconds) Obtained from Fitting the Differential Absorption Kinetics of the PA_n and PB_n Push−Pull Polyenes ($n = 2-5$, See Scheme 1) Dissolved in Solvents of Different Polarity, Viscosity, and Average Solvation Time[b]

		τ_i (ps)			
solvent	polyene series	$n = 2$	$n = 3$	$n = 4$	$n = 5$
cyclohexane	PB_n	160 ± 10	230 ± 10	120 ± 10	12 ± 3
$\epsilon = 2.02$ at 22 °C[c]	PA_n[d]	65 ± 5	6.0 ± 0.6	3.2 ± 1.0	3 ± 2
$\eta = 0.98$ cP at 20 °C[c]			100 ± 20	83 ± 5	15 ± 2
dioxane	PB_n	4 ± 1	3 ± 1	5 ± 1	4.0 ± 0.8
$\epsilon = 2.2$ at 22 °C[c]		650 ± 50	550 ± 50	350 ± 20	55 ± 5
$\pi^* = 0.49$[e]	PA_n[d,f]	3 ± 1	2.5 ± 0.5	3 ± 1	2 ± 1
$\eta = 1.44$ cP at 15 °C[c]		480 ± 80	60 ± 30	275 ± 30	35 ± 5
$\langle\tau_s\rangle = 1.7$ ps[e]		650 ± 150			
tetrahydrofuran	PB_n	2.0 ± 0.5	1.9 ± 0.5	1.9 ± 0.5	3 ± 1
$\epsilon = 7.58$ at 22 °C[c]		220 ± 10	500 ± 50	400 ± 50	90 ± 10
$\pi^* = 0.55$[e]	PA_n	1.7 ± 0.5[d]	2 ± 0.5[d]	2.2 ± 0.5[d]	2 ± 1[d]
$\eta = 0.55$ cP at 20 °C[c]		870 ± 90	420 ± 80	370 ± 50	100 ± 10
$\langle\tau_s\rangle = 0.94$ ps[e]					
acetonitrile	PB_n	≤ 1	≤ 1	≤ 1	≤ 1
$\epsilon = 36$ at 22 °C[c]		25 ± 1	60 ± 5	135 ± 10	45 ± 5
$\pi^* = 0.66$[e]	PA_n	1 ± 0.5[d]	0.7 ± 0.4[d]	1 ± 0.4[d]	2 ± 1[d]
$\eta = 0.37$ cP at 30 °C[c]		70 ± 10	300 ± 60	300 ± 60	130 ± 15
$\langle\tau_s\rangle = 0.26$ ps[e]					
triacetin	PB_n	7 ± 2	6.5 ± 2.0	6 ± 2	5 ± 2
$\epsilon = 7.1$ at 20 °C[c]		410 ± 80	970 ± 80	520 ± 80	93 ± 5
$\eta = 22$ cP at 20 °C[c]	PA_n	11 ± 2	17 ± 5	8 ± 4	7 ± 3
$\langle\tau_s\rangle = 49.5$ ps[g]		1300 ± 200	1500 ± 500	600 ± 100	90 ± 30

[a] Calculated from values at different wavelengths across the transient absorption spectra and in repeated experiments. [b] The fits were done by convoluting the pump−probe cross-correlation function (assumed to be a Gaussian) with a sum of exponentials and a step function, which describes the residual signal at long delays. The solvents are characterized by their polarity (dielectric constant ϵ and π^* parameter), viscosity η and average solvation time $\langle\tau_s\rangle$. [c] From ref 71. [d] From ref 38. [e] From ref 51. [f] From ref 36. [g] From ref 53.

sum of two to three exponentials and a step function. The time constants, averaged over results obtained at several selected wavelengths, are given in Table 1.

THF and Acetonitrile. A short-time dynamics similar to that in dioxane is found in THF and in acetonitrile. The TIP in the stimulated-emission band is less obvious, however, in particular for the short chains (PB_2 and PB_3). The amplitude of the delayed rise of the stimulated-emission band of PB_4 and PB_5 is also smaller. Spectra in THF are given for PB_3 in Figure 3 (left) for both short and long pump−probe delays. At long delays, the formation of a photoproduct is less obvious. However, a very weak residual absorption band of PB_3 is observed around 750 nm in acetonitrile. For PB_2, although the stimulated-emission band decays faster than in the case of PB_3, the spectra do not show clear evidence for the formation of a photoproduct, both in THF and in acetonitrile. For PB_4 and PB_5 in both THF and acetonitrile, a broad and weak absorption remains above 800 nm, like in dioxane. Time constants obtained from the fits at selected wavelengths (Table 1) definitely show that both the solvent properties and the polyenic chain length control the relaxation kinetics. It is, for example, seen that the excited-state decay time of PB_5 remains smaller than 100 ps in the three low-viscosity polar solvents examined here, and that solvent-induced differences reach, at most, a factor of 2. On the other hand, the excited-state decay of PB_2 is strongly solvent-dependent and can be as long as 650 ps in dioxane.

3.3. Picosecond Transient Absorption Spectra in Triacetin. Triacetin was chosen because its dielectric constant is close to that of THF, while its viscosity and average solvation time are 40 and 53 times larger, respectively (Table 1). Figure 3 shows a comparison of the short- and long-time dynamics of PB_3 in these two solvents. In triacetin, a progressive red shift of the stimulated-emission band is clearly seen on the short time-scale, explaining why no TIP is observed, although the delayed increase lasts up to several tens of picoseconds. This shift also exists in THF, on a much shorter time scale and with a much smaller amplitude. In triacetin on the long time-scale, the red shift of the stimulated-emission band continues for several hundred picoseconds while the band decays. Its final position, around 770 nm, equals the position of the same band reached in THF after 5 ps. The transient absorption changes observed for PB_3 are slower in triacetin than in THF (Table 1). Similar observations are made for PB_2. For PB_4, only the short-time dynamics appears to vary between THF and triacetin. Little effect is observed for PB_5. Although triacetin affects the transient absorption kinetics of the four polyenes differently, a similar red shift of the stimulated-emission band is observed in all cases. Figure 4 compares the shifts of the stimulated-emission maxima of PB_2 and PB_3 to those of PA_2 and PA_3. The plot demonstrates that the dynamics is independent of the donor group and the chain length. The time constants obtained from a biexponential fit are 3.5 ± 0.7 ps and 90 ± 10 ps, each one having a 50% weight.

3.4. Nanosecond to Millisecond Behavior in Selected Cases. In order to characterize the nature of the long-lived photoproducts detected in the experiments described above, we carried out a few experiments with time delays extending up to several tens of milliseconds by using two electronically synchronized subpicosecond laser systems.[38] Two kinds of remaining transient absorption bands were observed in the subpicosecond experiments: either a band that is mainly seen in the red edge of the ground-state absorption and is very likely overlapping it, or a broad band extending at the red side of the ground-state absorption up to 1000 nm. We chose to probe these photoproducts in the case of PB_2 in cyclohexane, which illustrates the first case, and in the case of PB_4 in dioxane, which illustrates the second case. Figure 5 shows that the 1.1-ns transient band observed for PB_2 in cyclohexane (Figure 1) is still present in the millisecond time range in a non-recirculating cell, suggesting that the band corresponds to a permanent photoproduct. Figure 5 shows that the photoproduct observed for PB_4 in dioxane is of a different nature: its lifetime is in the nanosecond range

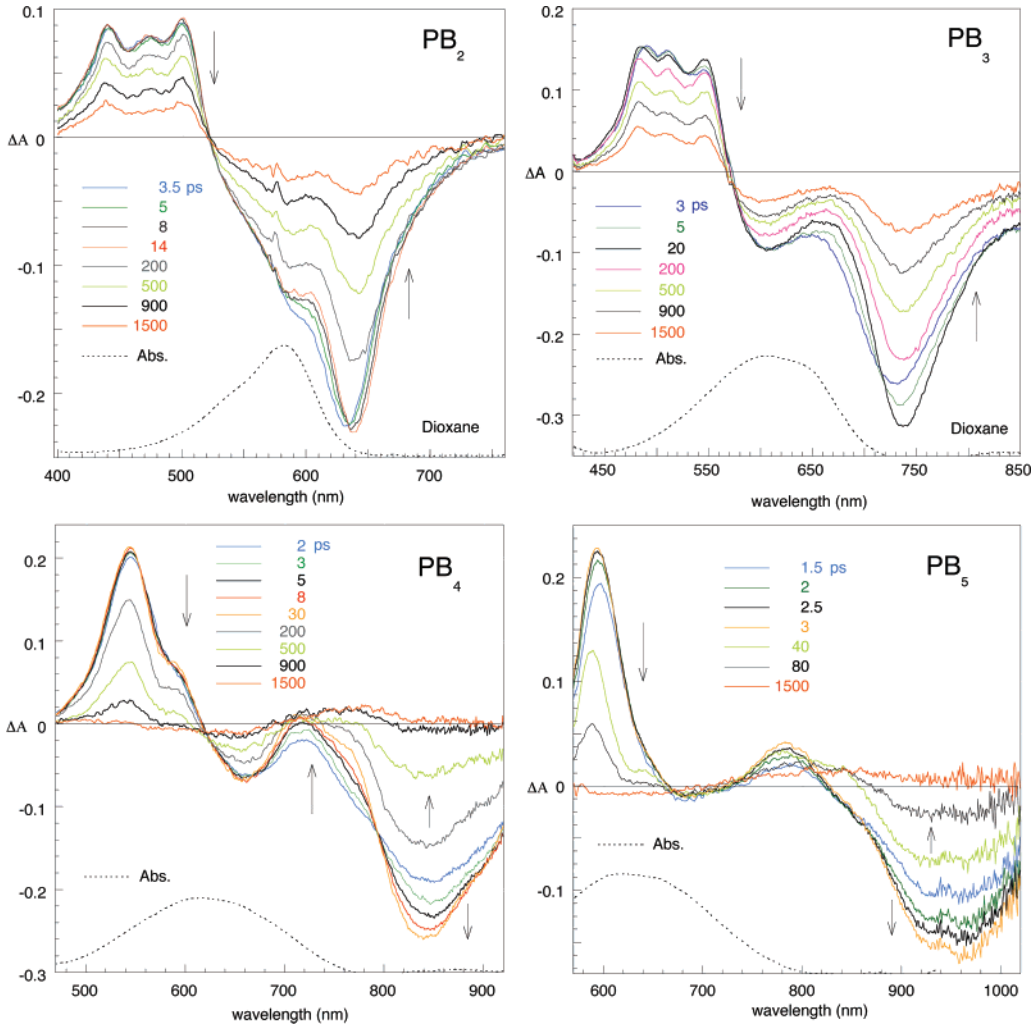

Figure 2. Differential absorption (ΔA) spectra of the PB_n polyenes in dioxane, upon subpicosecond excitation around 570−572 nm ($n = 2, 3, 4, 5$). The ground-state absorption spectrum is shown as a dotted line. On the short time-scale, a TIP is observed in the stimulated-emission region, while the maximum amplitude of the band increases. The arrows indicate the evolution of bands with increasing time.

and can be extended to microseconds under deaerated conditions. We have also studied PB_3 in dioxane because Figure 2 shows a TIP at 575 nm in the bleaching band while the excited-state decays. A photoproduct is indeed observed in the millisecond time scale and appears to be similar to that of PB_2 in cyclohexane.

4. Discussion

4.1. Solvent-Polarity-Controlled Ultrafast ICT. *Short-Time Dynamics in Polar Solvents.* The short-time dynamics of the differential absorption spectra found for the four PB_n in polar solvents dioxane (Figure 2), THF or triacetin (Figure 3), and acetonitrile is notably different in the case of the nonpolar solvent cyclohexane (Figure 1). In polar solvents, the early dynamics involves a delayed increase of the stimulated-emission band together with small changes in the transient absorption band, and a TIP is observed in a spectral region where stimulated emission is either dominant or the only contributor. The presence of a TIP in the gain band (Figures 2 and 3) is a strong indication that a fast reaction occurs in the excited state, with a precursor-successor relationship between the initial excited-state and a product species, both being emissive. We noted above that, for PB_2 and PB_3, the stimulated-emission TIP is less obvious in THF and acetonitrile than in dioxane, and, for PB_4 and PB_5, the amplitude of the observed stimulated-emission delayed rise is also smaller in THF and acetonitrile. This is consistent with the reaction being accelerated when the solvent polarity increases and eventually approaching or surpassing (see Table 1) the time resolution of our experiment (about 1 ps). It must be noted, however, that the TIP is no longer observed in triacetin, where a progressive red shift of the stimulated-emission band accompanies not only its delayed rise but also its decay. Figure 4, which compares the time-resolved red shifts of PA_2, PA_3, PB_2, and PB_3, suggests that this shift arises from solvation dynamics because it depends neither on the polyenic chain length nor on the donor group. These push−pull polyenes have been designed and characterized as efficient nonlinear optical chromophores with giant quadratic hyperpolarizabilities.[30,31] The estimated dipole moment change ($\Delta\mu$) upon S_0-S_1 excitation is as large as 42 D for the longest chain ($n = 5$) of the PA_n series in dioxane.[30,31] Although electrooptical data are not available for the PB_n series, one would expect a similar large photoinduced change of their dipole moment as was reported for a similar EDA polyenic series with the same donating moiety but having a dicyanovinyl moiety as the electron-accepting end group instead.[52] Upon femtosecond optical excitation, the excited-state population is left out of equilibrium with the surrounding solvent,[33−36] which then reorients around the new giant dipole. The dynamical shift plotted in Figure 4 can be fitted by two exponentials of the same weight and time constants

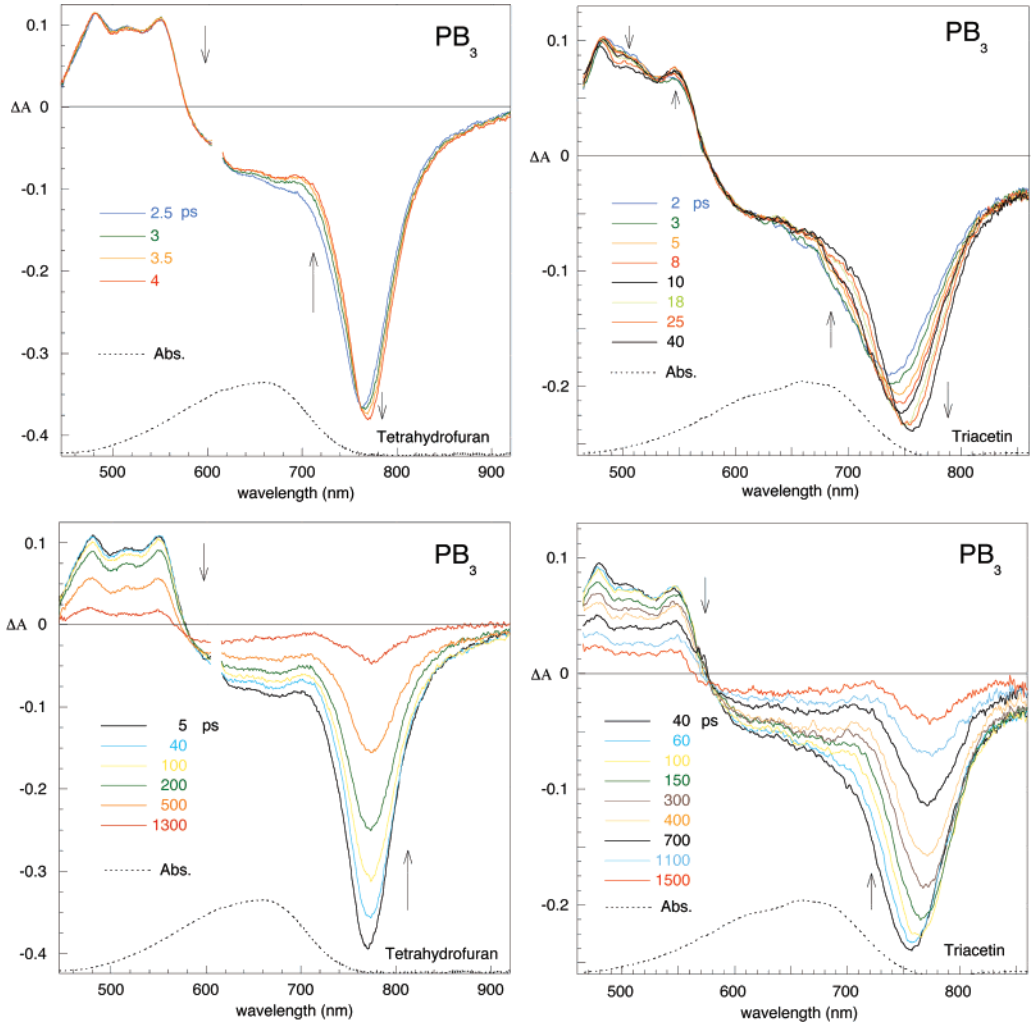

Figure 3. Differential absorption (ΔA) spectra of PB_3 in THF (left) and in triacetin (right), upon subpicosecond excitation at 610 and 571 nm, respectively. Scattered light from the excitation laser has been masked. On the short time-scale (up) a TIP is observed in the stimulated-emission region in THF, while, in triacetin, a continuous red shift of the peak accompanies the increase of the band. On the long time-scale (down), the red shift goes on while the band decays. The arrows indicate the evolution of bands with increasing time. The ground-state absorption spectrum is shown as a dotted line.

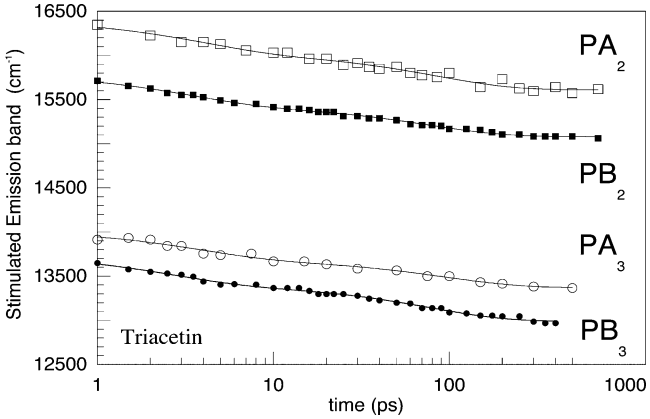

Figure 4. Comparison of the time-resolved red shifts of the stimulated-emission band maximum of PA_n and PB_n ($n = 2$ and 3) in triacetin. The evolution is biexponential, and the two time constants (3.5 and 90 ps, each one having a 50% weight) are identical, irrespective of the donor group and chain length. The observed dynamics is assigned to solvation dynamics.

of 3.5 and 90 ps. Both the resulting ~47 ps average solvation time and the 90 ps long time components are in excellent agreement with the solvation times measured by Chang and Castner[53] for triacetin (49.5 ps and 92 ps, respectively). This raises the question of whether we observed a genuine photoinduced reaction or merely spectral signatures of the solvation process. In the latter case, one would have to consider that the observation of the stimulated-emission TIP is fortuitous. It would be produced by a special modification of the shape of the stimulated-emission band as it shifts toward the red, which appears rather unlikely. Additionally, in dioxane, which has an average solvation time of 1.7 ps, one observes a TIP for about 20 ps (Figure 2). One may doubt that the weak (2% weight) 18-ps solvation-time component reported for this solvent[51] is responsible for this effect. We thus conclude that our data are best explained by the fast formation of an emissive, solvent-polarity-induced ICT state, in agreement with our previous interpretation for the PA series.[36,38] The role of the solvent reorganization as a reaction coordinate must, however, be addressed.

Role of External and Internal Coordinates in the ICT Reaction Path. The kinetics of the proposed ICT reaction can be analyzed from the time constants given in Table 1, where we gathered both the short- and long-time dynamics of the PB_n and PA_n series. These time constants are averaged values calculated from fits performed at different wavelengths and for different experiments. The short time constants obtained for the two series

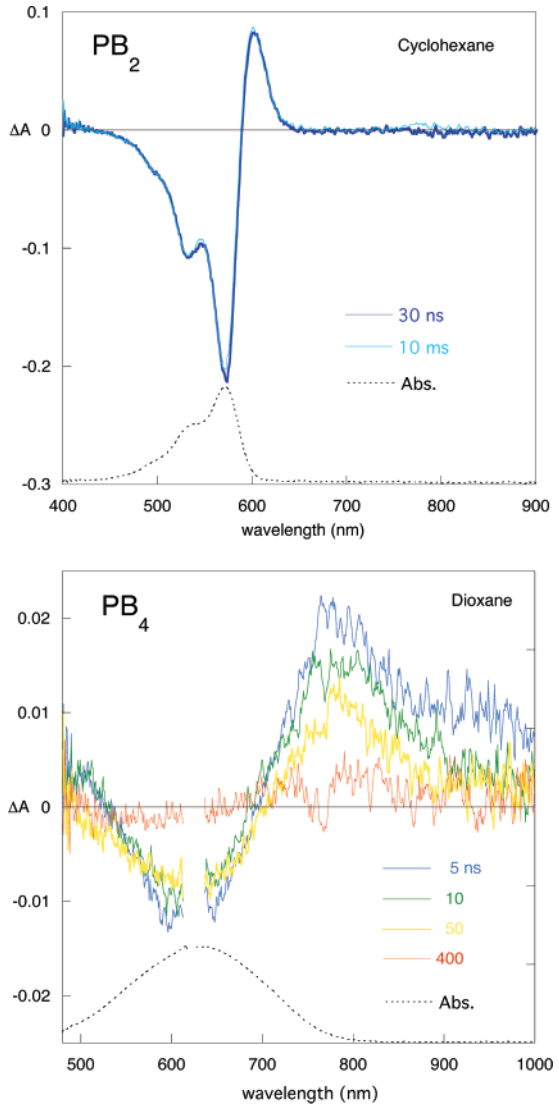

Figure 5. Differential absorption experiments carried out at delays extending up to milliseconds by using two electronically synchronized subpicosecond laser systems. The photoproduct observed for PB_2 in cyclohexane (top) still present in the millisecond time range in a non-recirculating cell is assigned to an isomer, whereas the one observed for PB_4 in dioxane (bottom), the lifetime of which lies in the nanosecond time scale in a non-degassed solution and in the microsecond time scale under a nitrogen flow (not shown), is assigned to the triplet state.

in polar solvents refer to the ICT reaction, whereas the long ones refer to the decay of the ICT state.

We now turn to the discussion of the effects of the solvent and chemical structure of the push−pull series on the rate of the initial ICT process. The analysis of the long-time decay rate and pathway will be done in section 4.2.

In Table 1, one notes that, for the four compounds of the PB series in fluid polar solvents, the ICT reaction time corresponds to 4 ± 1 ps in dioxane, 2 ± 1 ps in THF, and within the time resolution of our experiment in acetonitrile. For the PA_n series,[36] the reaction occurs in approximately 3 ps in dioxane, 2 ps in THF, and 1 ps in acetonitrile, except for PA_5, for which the initial reaction time is approximately 2 ps in all solvents. The main trend is thus that the ICT rate in the PB_n series is comparable to that in the PA_n series, in spite of the stronger electron-donor end group of the PB_n. Because of this stronger donor group, one might have expected a lower energy of the PB_n ICT state as compared to that of PA_n in a given solvent, implying an ICT reaction profile with a lower barrier and thus faster ICT kinetics. One should thus raise the question of the coordinates involved in the observed reaction. A two-dimensional theory, involving both solvent reorganization and internal twisting, was developed with success by Kim and Hynes[39] for the photoinduced barrier-activated TICT-state formation of DMABN. The calculated reaction rates were found to be in excellent agreement with the experimental results in acetonitrile, methanol, and ethanol.[54] In acetonitrile, the model predicts that the barrier crossing is mainly along the internal coordinate, whereas, in methanol, the solvent coordinate is predominant. Such a two-dimensional model is probably necessary to describe the photodynamics of the present push−pull compounds. The fact that the ICT rate in the PA_n and PB_n in dioxane, THF, and acetonitrile is slightly slower than the average solvation time may be considered as an indication that an intramolecular coordinate is involved in the barrier crossing, beside solvation. Additional arguments in favor of an intramolecular coordinate in the present study may be found by comparing the short time components of the PA_n and PB_n series in THF and triacetin, which have the same polarity but different viscosities (Table 1). In all cases, the ICT process is slowed down in the viscous triacetin, however, with a larger effect for the PA_n: the ICT time is 2−3 ps for both series in THF, whereas it increases up to 7−17 ps for the PA_n and to 5−7 ps for the PB_n in triacetin. The larger viscosity effect observed for the PA_n can be explained in two ways. According to the Grote−Hynes theory,[40] the reaction rate in a given solvent is not only determined by the barrier height but also by the barrier frequency (ω_b), that is, the shape of the parabolic barrier along the reaction path. The Grote−Hynes theory predicts that barrier crossing rate in solution is determined by the events occurring in the solvent on the time scale of the order of the reciprocal of the barrier frequency (ω_b^{-1}). It thus predicts viscosity effects, that is, "slow" hydrodynamic friction effects, on low-frequency barriers.[40] PA_n could be more sensitive to viscosity than PB_n because of a lower barrier frequency for the reaction. This might in turn be correlated to a lower intramolecular torsional frequency, the torsional motion being the rotation of the electron-donor group in the present case. As a matter of fact, the dibutylaniline donor group of the PA_n has a larger size/mass and less compact structure than the julolidine donor group of the PB_n. It is thus likely that the torsional frequency is lower for the PA_n than for the PB_n. Alternatively, even if the barrier frequency of both PA_n and PB_n is low enough to allow full sensitivity to solvent viscosity, the larger dibutylaniline group is likely to experience more hydrodynamic friction along its rotation motion than the julidino group.

Cyanine Structure of the ICT State. In our previous publications on the PA_n,[36,38] we noted that the stimulated-emission band in polar solvents exhibits a red shift of ∼110 nm per added double bond in the polyenic chain. This indicates that the ICT state reached from the initial excited-state has a cyanine structure,[55−57] that is, a π-electron delocalization over the full length of the chain, no bond-length alternation, and a planar rigid geometry. Figure 6 shows the red shift of the stimulated-emission maximum once the ICT state is formed, that is, at 14 ps in dioxane, 5 ps in THF, and 2−5 ps in acetonitrile. A regular shift of 110 ± 10 nm of the stimulated-emission band is observed in the three solvents when the chain length increases (this could have also been deduced from steady-state measurements with a fluorimeter working in the far-red spectral range). This regular shift is not observed for the steady-state absorption spectra, where the red shift saturates for $n \geq 3$. Instead a broadening is observed, possibly indicating that different

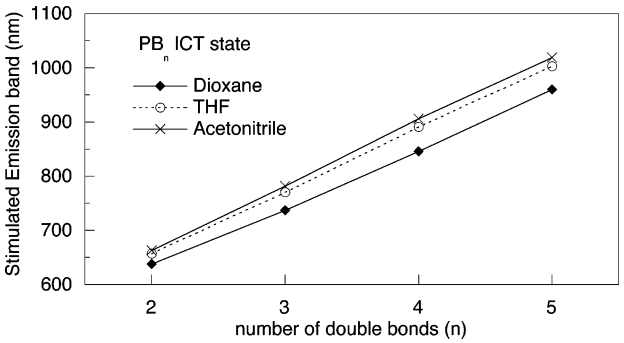

Figure 6. Red shift of the stimulated-emission band maximum of PB_n, measured at about 14 ps in dioxane, 5 ps in THF, and 2−5 ps in acetonitrile, upon increasing chain length (2−5 double bonds). This maximum belongs to the ICT state. A regular red shift of ∼110 nm is observed in the three solvents, indicating that the ICT state has a cyanine-like structure.

conformers of the longest chain coexist. Another similarity with the PA_n series is the small polarity effect on the stimulated-emission maximum.[36] From Figure 6 one can indeed estimate a shift of less than 800 cm^{-1} from dioxane to acetonitrile. We had previously stressed that a polarity-independent emission peak position was indeed expected for cyanine-like structures since they correspond, both in the ground and excited states, to a 50/50% mixture of the neutral and zwitterionic valence bond forms used in some theoretical models[33,34] to describe these compounds.

The formation of such a cyanine-like ICT state is very likely to involve not only geometrical changes along the polyenic chain but also twisting of the terminal groups in order to reach the expected flat, fully conjugated configuration. This brings further support to the idea that the fast ICT process in polar solvents probably involves the torsion of the electron-donor group. The solvation dynamics observed while the ICT state is formed shows that the initially excited state is more polar than the ground state. On the other hand, the observation that the ICT reaction is promoted and accelerated by a polar environment is a strong indication that the transient cyanine-like ICT state is even more polar than the initially excited state. This explains why the ICT state is not observed in nonpolar cyclohexane, where it is expected to have a higher energy than the initially excited state. In the case of the PA_n series, electro-optical absorption measurements provided direct experimental evidence for a large excitation-induced change of the dipole moment,[30,31] as mentioned above in the first subsection of section 4.1. In dioxane, the reported ground-state dipole moment is about 9 D, independently of the chain length, whereas the corresponding values in the Franck−Condon excited-state increase from 21.8 D ($n = 2$) to 51.4 D ($n = 5$).[31] Under the assumption of a maximum charge-separation between the donor and the acceptor end groups, the dipole moments of the cyanine-like ICT state are roughly estimated as ∼40 D ($n = 2$) to ∼80 D ($n = 5$). Obviously, these values are much higher than the dipole moments found for the locally excited states.

4.2. Isomerization or Crossing to the Triplet State: Role of the Polyenic Chain Length. By comparing the long time-dynamics of the PA_n series in cyclohexane and dioxane, we had previously demonstrated that the excited-state population experiences a change in its relaxation route as the polyenic chain length increases.[38] The change was observed for $n = 3$ in both solvents, however, with a qualitative difference. In dioxane, the ICT-state relaxation changes from cis−trans photoisomerization ($n = 2$) to intersystem crossing ($n = 3$), whereas, in cyclohexane, the relaxation path of the initially excited state changes from cis−trans photoisomerization ($n = 2$) to direct relaxation to the ground state ($n = 3$), then intersystem crossing ($n = 4$). In dioxane, the intermediate case with a direct relaxation to the ground state is not observed. We will propose here relaxation pathways for the PB_n series.

Long-Time Dynamics in Polar Solvents. The lifetime of the ICT state of the PB_n in polar solvents is given by the long time component shown in Table 1. One sees that, except in dioxane, the lifetime increases for n increasing from 2 to 3, then decreases for longer chains, except in acetonitrile, where the turning point is observed at $n = 4$. For a given chain length, polarity and viscosity effects can be seen. Viscosity effects at constant polarity can be observed by comparing THF and triacetin. We see that the ICT-state lifetime of the shortest chains ($n = 2, 3$) increases by a factor of 2 in the more viscous solvent, while the ICT-state lifetime of the longest chains ($n = 4, 5$) is not sensitive to viscosity within experimental error. As far as polarity is concerned, one observes that the ICT-state lifetime decreases with increasing polarity for PB_2 and PB_3 (larger effect on PB_2), while PB_4 and PB_5 exhibit a different behavior, with a maximum value in THF. This observation strongly indicates that the relaxation pathway of PB_2 and PB_3 differs from PB_4 and PB_5. Figure 5 shows the absorption band of the long-lived photoproduct observed for PB_4 in dioxane. Its lifetime, which is in the nanosecond range under aerated conditions and can be extended to microseconds under a nitrogen flow, is characteristic of a triplet state. The photoproduct found for PB_3 in the same solvent is a permanent product, which we assign to a cis−trans photoisomer. A change from photoisomerization to intersystem crossing thus occurs at $n = 4$ for the ICT-state relaxation of the PB_n series in dioxane. The different viscosity effects observed on the ICT lifetime in THF and triacetin allow us to conclude that the route change holds true in these solvents. The correlation with viscosity for the short chains is indeed compatible with photoisomerization, while the absence of a viscosity effect on the long chains agrees with crossing to the triplet state. In acetonitrile, the residual transient spectra of PB_4 and PB_5 are quite similar (not shown) to those observed in dioxane and THF. One may thus hypothesize that crossing to the triplet also occurs for these long-chain polyenes in acetonitrile. For the short chains, a small residual absorption indicates the formation of a photoproduct at $n = 3$, but this is not clear at $n = 2$, although the lifetime of the ICT-state of PB_2 is quite short (25 ps). Direct relaxation to the ground state might compete with photoisomerization in the latter case. The observed increase of the ICT-state lifetime from $n = 2$ to 3 is expected, however, if photoisomerization occurs.

The decrease of the photoisomerization rate with increasing n observed for PB_2 and PB_3 in THF, triacetin, and possibly in acetonitrile is in agreement with reports on substituted polyenes[58,59] and symmetrical cyanines[60] (see also references in ref 38). Acceleration of the reaction in polar solvents is a strong indication that the dipole moment of the excited state in the S_1/S_0 crossing region is larger than that of the ICT state. This has also been reported for polymethine cyanines.[60,61] On the other hand, the crossing to the triplet state may become more favorable while the chain length increases as a result of the increase of the barrier to isomerization, even in highly polar solvents.

From Table 1, one sees that the ICT-state lifetimes of the PA_n in a given solvent follow a trend similar to that of the lifetimes of the PB_n ICT-state, with a maximum for $n = 3$, except in THF, where the lifetime keeps decreasing when n increases. The ICT-state lifetime of PA_2 and PA_3 in triacetin is

1.5 to 3 times larger than in THF, which is compatible with a cis−trans photoisomerization reaction. PA_4, however, which is expected to undergo intersystem crossing as in dioxane, shows some unexpected sensitivity to viscosity. This viscosity effect may indicate that crossing to the triplet state occurs while the ICT-state population propagates along the isomerization coordinate. The influence of the solvent polarity is also less regular than in the case of PB_n, which might result from the fact that PA_n bears a weaker electron donor end group.

Long-Time Dynamics in Cyclohexane. In cyclohexane, although the transient ICT state is not formed, one also observes an increase of the excited-state lifetime of the PB_n from $n = 2$ to 3 followed by a decrease for further increase of the chain length (Table 1). The trend is similar to what we observed for the PA_n, although, in the latter case, the kinetics were nonexponential (still obscure to us).[38] Most of the measured lifetimes are larger for the PB_n series bearing the stronger electron-donor group. From experiments carried out in the nanosecond to millisecond time scale (Figure 5), one can assign the permanent photoproduct of PB_2 to an isomer, as for PA_2.[38] The fact that PB_2 photoisomerizes more slowly than PA_2 is likely due to the photoisomerization barrier being raised by the presence of the stronger electron donor. In the PA series, the relaxation route changes to intersystem crossing for $n = 4$, while relaxation down to the initial ground state is more favorable for PA_3.[38] Figure 1 demonstrates that, unlike PA_3, a photoproduct is formed for PB_3. As we have not carried out experiments on the nanosecond to millisecond time scale for $PB_{3,4,5}$ in cyclohexane, the nature of the product observed in these cases is not certain. By analogy with the results in polar solvents, described above, the increase of lifetime from PB_2 to PB_3 nevertheless suggests that photoisomerization also occurs in PB_3, whereas the shorter lifetimes of PB_4 and PB_5 evoke intersystem crossing. Examination of the residual absorption spectra of Figure 1 might bring support to this hypothesis because the transient absorption spectrum of PB_4 and PB_5 have a similar shape, with a relatively sharp maximum around 780 and 800 nm, respectively, which is not observed for PA_2 and PB_3. These results give definitive evidence that the polyenic chain length, the chemical nature of the end group, and the solvent polarity affect the relative position of the different excited-state surfaces, their intersections, and thus the branching ratios.

4.3. Similarity with Carbonyl Carotenoids. The influence of the chemical structure on the excited-state surface topologies and on the nature and location of the relaxation funnels is one of the most fundamental questions in photochemistry. We previously thoroughly situated[38] our findings on the successive solvent-controlled and chain-length-controlled branchings of the excited-state population propagation of the PA_n within the context of substituted polyenes, cyanines, and carotenoids. The main question raised for polyenes and carotenoids concerns the role of the chain length on the relative location of the 1^1B_u and 2^1A_g lowest excited states, on their coupling, and on their deactivation pathway and kinetics. Since substitution changes the symmetry properties of the molecule, the questions raised for the present push−pull polyenes are slightly different. The photochemical behavior of substituted carotenoids, which was shown to depend strongly on the EDA character of the terminal groups and on the length of the polyenic chain connecting them, offers a better basis for comparison.[5,41,42,62,63] The implication of the first triplet state as a photoproduct in carotenoids[5] and as an intermediate in the photoisomerization of some cyanines and substituted polyenes[64−66] is also relevant. An ultrafast process involving a two-mode intramolecular motion toward a conical intersection has been proposed for the cis−trans isomerization of the retinal protonated Schiff base involved in the vision process and of some polymethine cyanines dyes.[60] More recently, the influence of a polar and polarizable environment on charge-transfer processes at a conical intersection has been described by a diabatic free energy model yielding coupled surfaces as a function of both molecular coordinates and solvent coordinates and illustrated for the S_1/S_0 crossing in protonated Schiff bases.[67] It was shown that solvent motion is necessary for reaching the conical intersection. All these aspects bring support to the involvement of concerted internal and external motion in defining the relaxation pathway of the present push−pull polyenes.

We wish, above all, to stress here that the short-time dynamics of both the PB_n and PA_n polyenes are relevant to understanding the photoinduced phenomena observed in carbonyl carotenoids such as peridinin[5,41−47] and are thus of interest to guide the design of artificial light-harvesting systems.[5,47] Peridinin, a carotenoid with a seven-double-bond polyenic chain including a lactone ring, is the main light-harvesting pigment in a chlorophyll complex found in photosynthetic dinoflagellates.[5] It is one of the best models of light harvesters, with a strong absorption in the blue-red region and close to 100% energy transfer to chlorophyll.[68] One singularity of this carotenoid is that the energy transfer proceeds from an ICT state rapidly formed from the lowest-excited singlet state, following ultrafast internal conversion from the excited, optically allowed, S_2 state.[5,41] In very recent years, such an ICT process has also been observed for other carbonyl carotenoids,[69,70] the structure of which contains electron-withdrawing substituents similar to the carbonyl group in peridinin. The main arguments in favor of the ICT-state formation from the S_1 state of peridinin were that the S_1-state lifetime depends strongly on solvent polarity.[41,62] It ranges from 160 ps in nonpolar solvents to a few picoseconds in polar solvents.[41,42,62] In addition, stimulated emission of the ICT state was observed in the IR spectral range (∼1000 nm in ethanol).[42] This is quite similar to what we observed for the present PA_n and PB_n push−pull polyenes. The present study not only refines our knowledge of the excited-state properties of push−pull systems designed for their nonlinear optical properties, but it is also of primary importance for understanding the complex excited-state behavior of efficient natural light-harvesters such as carbonyl carotenoids.

5. Conclusion

The excited-state decay time and relaxation pathway of four push−pull polyenes (PB_n), bearing a julolidine electron donor, a diethylthiobarbituric acid electron acceptor, and $n = 2-5$ double bonds in the chain, have been studied by subpicosecond absorption spectroscopy in cyclohexane, dioxane, THF, acetonitrile, and triacetin. The results are compared to those obtained, and already partially published,[36,38] for analogues (PA_n) bearing a weaker (also larger and less compact) electron donor, a dibutylaniline group. For both series, ICT leading to an excited cyanine-like structure (fully conjugated with no bond-length alternation) is observed in all polar solvents at a solvent-dependent rate. Similar kinetics are observed for the two series, in spite of the difference of their electron-donor end group. In fluid polar solvents, the charge-transfer time is, at most, 5 ps in the less polar solvent, dioxane, and ≤1 ps in the more polar solvent, acetonitrile. Charge-transfer time increases with average solvation time but always remains slightly larger. These observations are interpreted as an indication that both the solvent reorganization and a torsional motion of the donor group are

involved in the charge-transfer reaction. At constant polarity, the fact that the reaction is slower in the viscous solvent triacetin than it is in the fluid solvent THF supports this interpretation. A shift of the stimulated-emission band is particularly seen in triacetin, during both the growth and the decay of the ICT state. It is shown to reflect solvation dynamics, triggered by the large dipole moment change occurring upon excitation. A further increase of the dipole moment is proposed in the cyanine-like ICT state and thought to explain why the reaction is not observed in the nonpolar cyclohexane.

Both the chain length and solvent polarity are found to control the excited-state relaxation pathway and decay time. The general trend is that the shorter chains photoisomerize in polar solvents, whereas the longer ones undergo crossing to the triplet state, with a clear difference in viscosity effects. The donor character of the electron-donor group may be involved in the change of relaxation route, which appears for $n = 3$ in the PA_n series and in $n = 4$ in the PB_n series. In cyclohexane, the intermediate regime with a direct relaxation to the ground state is not observed for the PB_n series, while it was seen for PA_3. The results clearly illustrate that photoinduced reactions in push−pull polyenes are controlled by parameters such as static and dynamic properties of the solvent, chemical nature and size of the end groups, and conjugated-chain length and flexibility. In addition, the characterization of the initial fast ICT reaction from the first excited state is believed to be of interest for a better understanding of the photophysics of carbonyl carotenoids.

Acknowledgment. Financial support from CNRS (Chemistry Department) GDR 1017, Laboratoire de Photophysique Moléculaire (Orsay), and Department of Chemistry of Ecole Normale Supérieure (Paris) is acknowledged. The authors wish to thank J. T. Hynes who was with them as a Visiting Scientist while these experiments were carried out. They wish to acknowledge his teaching and profound views in so many fields. They also want to thank him for fruitful discussions they have had with him over the past years.

References and Notes

(1) Fabian, J.; Nakazumi, H.; Matsuoka, M. *Chem. Rev.* **1992**, *92*, 1197−1226.
(2) Mishra, A.; Behera, R. K.; Behera, P. K.; Mishra, B. K.; Behera, G. B. *Chem. Rev.* **2000**, *100*, 1973−2011.
(3) Koyama, Y.; Kuki, M.; Andersson, P. O.; Gillbro, T. *Photochem. Photobiol.* **1996**, *63*, 243−256.
(4) Frank, H. A. *Arch. Biochem. Biophys.* **2001**, *385*, 53−60.
(5) Polivka, T.; Sundström, V. *Chem. Rev.* **2004**, *104*, 2021−2071.
(6) Kochendoerfer, G. G.; Mathies, R. A. *Israel J. Chem.* **1995**, *35*, 211−226.
(7) Mathies, R. A.; Brito Cruz, C. H.; Pollard, W. T.; Shank, C. V. *Science* **1988**, *240*, 777−779.
(8) Gai, F.; Hasson, K. C.; McDonald, J. C.; Anfinrud, P. A. *Science* **1998**, *279*, 1886−1891.
(9) Herbst, J.; Heyne, K.; Diller, R. *Science* **2002**, *297*, 822−825.
(10) Schenkl, S.; van Mourik, F.; van der Zwan, G.; Haacke, S.; Chergui, M. *Science* **2005**, *309*, 917−920.
(11) Oudar, J.-L. *J. Chem. Phys.* **1977**, *67*, 446−457.
(12) Oudar, J.-L.; Chemla, D. S. *J. Chem. Phys.* **1977**, *66*, 2664−2668.
(13) Barzoukas, M.; Blanchard-Desce, M.; Josse, D.; -M, L. J.; J, Z. *Chem. Phys.* **1989**, *133*, 323−329.
(14) Puccetti, G.; Blanchard-Desce, M.; Ledoux, I.; Lehn, J.-M.; Zyss, J. *J. Phys. Chem.* **1993**, *97*, 9385−9391.
(15) Marder, S. R.; Cheng, L. T.; Tiemann, B. G.; Friedly, A. C.; Blanchard-Desce, M.; Perry, J. W.; Skindhoj, J. *Science* **1994**, *263*, 511−514.
(16) Lu, D.; Chen, G.; Perry, J. W.; Goddard, W. A., III. *J. Am. Chem. Soc.* **1994**, *116*, 10679−10685.
(17) Chen, G.; Lu, D.; Goddard, W. A., III. *J. Chem. Phys.* **1994**, *101*, 5860−5864.
(18) Blanchard-Desce, M.; Lehn, J.-M.; Barzoukas, M.; Ledoux, I.; Zyss, J. *Chem. Phys.* **1994**, *181*, 281−289.
(19) Blanchard-Desce, M.; Runser, C.; Fort, A.; Barzoukas, M.; Lehn, J.-M.; Bloy, V.; Alain, V. *Chem. Phys.* **1995**, *199*, 253−261.
(20) Marder, S. R.; Torruellas, W. E.; Blanchard-Desce, M.; Ricci, V.; Stegeman, G. I.; Gilmour, S.; Brédas, J.-L.; Li, J.; Bublitz, G. U.; Boxer, S. G. *Science* **1997**, *271*, 1233−1236.
(21) Dick, B.; Stegeman, G.; Twieg, T.; Zyss, J. *Chem. Phys.*, **1999**, *245*, 1−565.
(22) Alain, V.; Thouin, L.; Blanchard-Desce, M.; Gubler, U.; Bosshard, C.; Günter, P.; Muller, J.; Fort, A.; Barzoukas, M. *Adv. Mater.* **1999**, *11*, 1210−1214.
(23) Alain, V.; Blanchard-Desce, M.; Ledoux-Rak, I.; Zyss, J. *Chem. Commun.* **2000**, 353−354.
(24) Ahleim, M.; Barzoukas, M.; Bedworth, P. V.; Blanchard-Desce, M.; Fort, A.; Hu, Z.-Y.; Marder, S. R.; Perry, J. W.; Runser, C.; Staehelin, M.; Zysset, B. *Science* **1996**, *271*, 335−337.
(25) Bublitz, G. U.; Ortiz, R.; Runser, C.; Fort, A.; Barzoukas, M.; Marder, S. R.; Boxer, S. G. *J. Am. Chem. Soc.* **1997**, *119*, 2311−2312.
(26) Moreaux, L.; Sandre, O.; Blanchard-Desce, M.; Mertz, J. *Opt. Lett.* **2000**, *25*, 320−322.
(27) Moreaux, L.; Pons, T.; Dambrin, V.; Blanchard-Desce, M.; Mertz, J. *Opt. Lett.* **2003**, *28*, 625−627.
(28) Dombeck, D. A.; Blanchard-Desce, M.; Webb, W. W. *J. Neurosci.* **2004**, *24*, 999−1003.
(29) Dombeck, D. A.; Sacconi, L.; Blanchard-Desce, M.; Webb, W. W. *J. Neurophys.* **2005**, *94*, 3628−3636.
(30) Blanchard-Desce, M.; Alain, V.; Bedworth, P.; Marder, S.; Fort, A.; Runser, C.; Barzoukas, M.; Lebus, S.; Wortmann, R. *Chem.—Eur. J.* **1997**, *3*, 1091−1104.
(31) Blanchard-Desce, M.; Alain, V.; Midrier, L.; Wortmann, R.; Lebus, S.; Glania, C.; Krämer, P.; Fort, A.; Muller, J.; Barzoukas, M. *J. Photochem. Photobiol. A: Chem.* **1997**, *105*, 115−121.
(32) Blanchard-Desce, M.; Barzoukas, M. *J. Opt. Soc. Am. B* **1998**, *15*, 302−307.
(33) Thompson, W. H.; Blanchard-Desce, M.; Alain, V.; Muller, J.; Fort, A.; Barzoukas, M.; Hynes, J. T. *J. Phys. Chem. A* **1999**, *103*, 3766−3771.
(34) Thompson, W. H.; Blanchard-Desce, M.; Hynes, J. T. *J. Phys. Chem. A* **1998**, *102*, 7712−7722.
(35) Laage, D.; Thompson, W. H.; Blanchard-Desce, M.; Hynes, J. T. *J. Phys. Chem. A* **2003**, *107*, 6032−6046.
(36) Plaza, P.; Laage, D.; Martin, M. M.; Alain, V.; Blanchard-Desce, M.; Thompson, W. H.; Hynes, J. T. *J. Phys. Chem. A* **2000**, *104*, 2396−2401.
(37) Moran, A. M.; Delbecque, C.; Myers, Kelley, A. *J. Phys. Chem. A* **2001**, *105*, 10208−10219.
(38) Laage, D.; Plaza, P.; Blanchard-Desce, M.; Martin, M. M. *Photochem. Photobiol. Sci.* **2002**, *1*, 526−535.
(39) Kim, H. J.; Hynes, J. T. *J. Photochem. Photobiol. A: Chem.* **1997**, *105*, 337−343.
(40) Grote, R. F.; Hynes, J. T. *J. Chem. Phys.* **1980**, *73*, 2715−2732.
(41) Bautista, J. A.; Connors, R. E.; Bangar Raju, B.; Hiller, R. G.; Sharples, F. P.; Gosztola, D.; Wasielewski, M. R.; Frank, H. A. *J. Phys. Chem. B* **1999**, *103*, 8751−8758.
(42) Zigmantas, D.; Polivka, T.; Hiller, R. G.; Yartsev, A.; Sundström, V. *J. Phys. Chem. A* **2001**, *105*, 10296−10306.
(43) Zigmantas, D.; Hiller, R. G.; Yartsev, A.; Sundström, V.; Polivka, T. *J. Phys. Chem. B* **2003**, *107*, 5339−5348.
(44) Vaswani, H. M.; Hsu, C.-P.; Head Gordon, M.; Fleming, G. R. *J. Phys. Chem. B* **2003**, *107*, 7940−7946.
(45) Papagiannakis, E.; Larsen, D. S.; van Stokkum, I. H. M.; Vengris, M.; Hiller, R. G.; van Grondelle, R. *Biochemistry* **2004**, *43*, 15303−15309.
(46) Premvardhan, L.; Papagiannakis, E.; Hiller, R. G.; van Grondelle, R. *J. Phys. Chem. B* **2005**, *109*, 15589−15597.
(47) Polivka, T.; Pellnor, M.; Melo, E.; Pascher, T.; Sundström, V.; Osuka, A.; Razi Naqvi, K. *J. Phys. Chem. C* **2007**, *111*, 467−476.
(48) Dai Hung, N.; Plaza, P.; Martin, M. M.; Meyer, Y. H. *Appl. Opt.* **1992**, *31*, 7046−7058.
(49) Kamlet, M. J.; Abboud, J.-L. M.; Abraham, M. H.; Taft, R. W. *J. Org. Chem.* **1983**, *48*, 2877.
(50) Reynolds, L.; Gardecki, J. A.; Frankland, S. J. V.; Horng, M. L.; Maroncelli, M. *J. Phys. Chem.* **1996**, *100*, 10337−10354.
(51) Horng, M. L.; Gardecki, J. A.; Papazyan, A.; Maroncelli, M. *J. Phys. Chem.* **1995**, *99*, 17311−17337.
(52) Blanchard-Desce, M.; Wortmann, R.; Lebus, S.; Lehn, J.-M.; Krämer, P. *Chem. Phys. Lett.* **1995**, *243*, 526−532.
(53) Chang, Y. J.; Castner, E. W., Jr. *J. Chem. Phys.* **1993**, *99*, 7289−7299.
(54) Changenet, P.; Plaza, P.; Martin, M. M.; Meyer, Y. H. *J. Phys. Chem. A* **1997**, *101*, 8186−8194.
(55) Fabian, J.; Hartmann, H. *Light Absorption of Organic Colorants*; Springer-Verlag: Berlin, 1980.
(56) Kuhn, H. *J. Chem. Phys.* **1949**, *17*, 1198−1212.
(57) Meyer, Y. H.; Pittman, M.; Plaza, P. *J. Photochem. Photobiol. A: Chem.* **1998**, *114*, 1−21.

(58) Bachilo, S. M.; Spangler, C. W.; Gillbro, T. *Chem. Phys. Lett.* **1998**, *283*, 235−242.

(59) Bartocci, G.; Galiazzo, G.; Gennari, G.; Marri, E.; Mazzucato, U.; Spalletti, A. *Chem. Phys.* **2001**, *272*, 213−225.

(60) Sanchez-Galvez, A.; Hunt, P.; Robb, M. A.; Olivucci, M.; Vreven, T.; Schlegel, H. B. *J. Am. Chem. Soc.* **2000**, *122*, 2911−2924.

(61) Momicchioli, F.; Baraldi, I.; Berthier, G. *Chem. Phys.* **1988**, *123*, 103−112.

(62) Frank, H. A.; Bautista, J. A.; Josue, J.; Pendon, Z.; Hiller, R. G.; Sharples, F. P.; Gosztola, D.; Wasielewski, M. R. *J. Phys. Chem. B* **2000**, *104*, 4569−4577.

(63) Zhangfei, H.; Gostztola, D.; Deng, Y.; Gao, G.; Wasielewski, M. R.; Kispert, L. D. *J. Phys. Chem. B* **2000**, *104*, 6668−6673.

(64) Waldeck, D. H. *Chem. Rev.* **1991**, *91*, 415−436.

(65) Görner, H. *J. Photochem.* **1982**, *19*, 343−356.

(66) Gurzadyan, G.; Görner, H. *Chem. Phys. Lett.* **2002**, *359*, 146−152.

(67) Burghardt, I.; Hynes, J. T. *J. Phys. Chem. A* **2006**, *110*, 11411−11423.

(68) Song, P. S.; Koka, P.; Prézelin, B. B.; Haxo, F. T. *Biochemistry* **1976**, *15*, 4422−4427.

(69) Wild, D. A.; Winkler, K.; Stalke, S.; Oum, K.; Lenzer, T. *Phys. Chem. Chem. Phys.* **2006**, *8*, 2499−2505.

(70) Kopczynski, M.; Ehlers, F.; Lenzer, T.; Oum, K. *J. Phys. Chem. A* **2007**, *111*, 5370−5381.

(71) Riddick, J. A.; Bunger, W. B. *Organic Solvents*, 3rd ed.; Wiley-Interscience: New York, 1970; Vol. II.